Current Trends in Technology and Science
ISSN: 2279- 0535. Volume: 3, Issue: 4(June-July 2014)

Classification of Ultrasonography Images of Human Fatty and Normal Livers using GLCM Textural Features

NiveditaNeogi
Assistant Professor, MeghnadSaha Institute of Technology, Kolkata, India,Email ID: nivedita.neogi@gmail.com

ArunbhaAdhikari
Associate Professor, West Bengal State University, Barasat, West Bengal, India, Email ID: arunabha.adhikari@gmail.com

Madhusudan Roy
Associate Professor, Saha Institute of Nuclear Physics, Kolkata, West Bengal, India, Email ID: roy.madhusudan@gmail.com

Abstract — A computer aided diagnosis methodology for identifying pathology of human liver using 11 statistical textural features extracted from ultrasonography of 14 fatty and 28 normal livers is presented. It was found that supervised classification could differentiate these two classes of data while unsupervised learning failed to achieve that. For supervised learning input sets were constructed in two alternative methods –i) Training set containing two third and test set one third of the data (conventional), ii) A representative training set generated using Self Organizing Map where entire data set was treated as test set. Both the inputs were used with and without Principal Component Analysis. The analysis shows that the Multi Layer Perceptron with conventional data set without pre-processing yields better results as compared to other paradigms.

Keyword — Fatty liver, Multi-Layer Perceptron, Principal Component Analysis, Self-Organizing Map,Ultrasonography.

1. INTRODUCTION

It is an involved issue in the field of clinical research to develop computer aided diagnostic (CAD) tool for identifying a pathological state of a human organ using its ultrasonogram (USG). The underlying objective of such research is to replace, if possible or at least minimize the role of a radiologist who classifies USG images using his/her perception as regards echo texture and echogenicity. Generally, texture features are extracted from the USG images of human liver either using first order statistics [1]-[2] or second order statistics [3]-[9] or both [10]. Other features based on Gabor filter and Law's spectra [11], Fractal Geometry and Wavelet Transform [12], Fractal analyses, Euler number and RF5 [13] are also used. There is no conclusive outcome of any study on identifyingthe texture featuresto be most appropriate for a given classification task. However mostcommonly used texture features of USG of human liver are extracted from Gray Level Co-Occurrence Matrices (GLCM) [3],[4],[6]-[9] for the classification of ultrasonic liver images.

To construct a CAD, it is imperative to choose a classifier which helps to classify the diseased and normal image with the best accuracy. There are two types of classifiers - statistical and neural network. Both are learned by unsupervised as well as supervised learning methods. Statistical unsupervised classifiers like K means clustering [14], statistical supervised classifier e.g. Support Vector Machine (SVM) [4]-[5], unsupervised neural network e.g. Self Organising Map (SOM) [11], supervised neural network like Multi Layer Perceptron (MLP) [3],[10] or combination of these [11] are used to classify USG human liver images. Other than liver, CAD is developed for different diseases of various human organs like breast cancer [15]-[17], muscles [17], coronary arteries [18], placenta [19]-[20], ovary [21], and atherosclerotic tissue [22]. From the literature, it is noticed that themost commonly used classifier is MLP. In many studies, SVM is usedwith good classification [23]-[24]. Besides, pre-processing of the input is important for good classification [17], [24], although there is no report available which shows explicitly the change in the classification efficiency due to pre-processing.

The present study uses statistical textural features extracted from USG images of diseased (fatty) and control (normal) human livers.Basically, there are three steps to construct the CAD: (i) selection the region of interest (ROI) from the USG image, (ii) feature extraction and (iii) classification of the image using a classifier. Selection of ROI is done in various ways: manual [25] or with the help of programming [14], [26]. The number of ROI is also variable at different studies. In the present study, small sub images of homogeneous pattern (excluding veins and ducts, patches etc.) were cropped by eye inspection in consultation with a radiologist.It is to note that for this work, 6 Haralick [27] and 5 non-Haralick features [28]-[30] based on GLCM [27] with 5 different pixel pair distances and 4 orientations were considered. SOM as an unsupervised classifier and MLP with error back propagation algorithm as a supervised classifier were applied. In case of

supervised learning, the total data set was divided into two parts- training and test. It is somewhat traditional that the size of training data set is always larger than the test data set, and generally, researchers divide the data set into train and test according to their own perception. However, if the test set is small then the performance measures are unreliable. Here we attempted to establish a new idea to create training data set by selecting representatives of the data by unsupervised learning method, namely, SOM. We dividedthe feature vectors derived from normal images into 20 clusters and consequent weight vectors were treated as representative feature vectors of the normal images. 20 representatives of the fatty images were also obtained by applying SOM separately on the fatty images. We constituted the training set by these 40 representatives feature vectors and the total data were used for test. The test set was large in this case and, therefore, the performance measures were more reliable. We worked with both types of training-test partition, traditional as well by our proposed method.In this study, we applied Principal Component Analysis (PCA) for pre-processing the feature values for understanding the necessity of pre-processing and observed the difference of the result by applying original as well as pre-processed data. Precisely, in this paper, we obtained results using MLP classifier with four paradigms- i) Training set containing two third and the test set one third data (conventional), ii) Training set generated using SOM, entire data set treated as test, iii) Conventional training set pre-processed with PCA and iv) and training set generated with SOM and pre-processed with PCA .

2. METHOD

2.1 IMAGE COLLECTION- Ultrasound images of human livers were acquired with a scanner (Siemens Sonoline Versa Plus), using broad bandwidth phased array convex transducer (ultrasound probe frequency was 3.5 MHz) and the image field size was 6 to 24 cm. Images were labelled as either fatty or normal by a radiologists (pathologically correlated image). Images have been captured with proper settings of the echo graphic instrument.

Fig 1.a

Fig 1.b

Figure 1 shows typical ultrasonograms of human fatty (1 a) and normal(1 b) liver. Rectangles show the non overlapping ROIs cropped manually from the USG avoiding the veins.

2.2 SAMPLE SELECTION- The data set consisted of 5 sub-images, each representing an ROI (see Fig 1b), from each ultra-sonogram of 28 patients having normal liver, thus resulting in a total of 140 inputs for normal livers. Similarly, to overcome the imbalance [31] 10 sub-images (Fig 1a) from each of 14 patients were cropped resulting in a total of 140 inputs for fatty livers.

2.3TEXTURALFEATURE DESCRIPTORS- Textural feature descriptors as devised by Haralick [27] based on Spatial Gray Level Dependence (SGLD), also known as GLCM were used for the study. The (i,j)th element of this

Current Trends in Technology and Science
ISSN: 2279- 0535. Volume: 3, Issue: 4(June-July 2014)

specifies the joint probability of occurrence of grey level pair (i,j) separated by a specified distance along a specified direction. GLCM matrices, in the present study, were computed from each of the sub-images for different neighbourhood pixel pair distances (NH= 1, 2, 3, 4 and 8) and directions (θ = 0°, 45°, 90°, 135°). To ease the computational efforts and avoid sparsity the sub-images were re-quantized to 16 gray levels. So for each sub-image 20 GLCM matrices were created. We calculated 11 features from each such GLCM matrix – 6 Haralick's features [27], namely, Contrast(Cont), Inverse element difference moment of order 2 (Ikmom), Angular Second Moment(ASM), Entropy (Ent),Correlation (Corr), Variance (var) and 3 other features, namely, Shade (shade),Promenance (prom), Inverse difference moment (IDM) [28], Maximum probability (Maxp)[29],Homogeneity (Homo) [30]. The explicit definitions of these features are described at table 1.

Table 1 describes the explicit definition of texture features used in present study. Symbols are explained in the text.

Maximum probability (Maxp)	$\max_{i,j}(c(i,j))$
Uniformity (Uni)	$\sum_i \sum_j (ci,j)^2$
Contrast (Const)	$\sum_i \sum_j (i-j)^2 c(i,j)$
Inverse element difference moment of order2 (IM2)	$\sum_i \sum_j c(i,j)/(i-j)^2 i\neq j$
Entropy (Ent)	$-\sum_i \sum_j c(i,j)\log_2 c(i,j)$
Homogeneity (Homo)	$\sum_i \sum_j c(i,j)/(1+\lvert i-j\rvert)$
Correlation (Corr)	$\frac{\sum_i \sum_j [(i-\mu_i)(j-\mu_j)c(i,j)}{\sigma_i \sigma_j}$
Variance(Var)	$\sum_i \sum_j (1-\mu)^2 c(i,j)$
Prominence (Prom)	$\sum_i \sum_j (i+j-\mu_i-\mu_j)^4 c(i,j)$
Shade(Shade)	$\sum_i \sum_j (i+j-\mu_i-\mu_j)^3 c(i,j)$
Inverse difference moment(IDM)	$\sum_i \sum_j c(i,j)/1+(i-j)^2$

Where **c** is the GLCM matrix, $\boldsymbol{\mu_i}$ and $\boldsymbol{\mu_j}$ are the mean values along row and column respectively, $\boldsymbol{\sigma_i}$ and $\boldsymbol{\sigma_j}$ are the standard deviations along row and column respectively. It is a usual practice [32-34] to average over the GLCM matrices of different NH and θ and extract the parameters from averaged GLCM. However, we did not perform this averaging in this paper and instead treated the features obtained from each of the above mentioned 20 GLCM matrices as independent yielding a total of 220 features. Nomenclature of the 20 independent datasets is shown in Table 2.

Table 2 Shows the nomenclature of 20 data sets used for this study and with their corresponding value of the NH, θ.

Dataset No	1	2	3	4	5	6	7	8	9	10
NH,θ	1,0	1,45	1,90	1,135	2,0	2,45	2,90	2,135	3,0	3,45
Dataset No	11	12	13	14	15	16	17	18	19	20
NH,θ	3,90	3,135	4,0	4,45	4,90	4,135	8,0	8,45	8,90	8,135

2.4 NORMALIZATION OF FEATURE COMPONENTS- For a given NH and θ, each of the above mentioned 11 feature components was tabulated from all the sub images and the maximum value for each component, considering both normal and fatty, was used to normalize that component.

3. RESULT AND DISCUSSION

Before attempting any classification we preferred to know whether if any feature component could readily distinguish between the classes. We used a parameter D_M(Equation 1).

$$D_M = \frac{|\bar{x}_1 - \bar{x}_2|}{s_1 + s_2} \qquad (1)$$

Numerical value of D_M, therefore, indicates how much the mean values are separated taking the individual variations in consideration. The prior distributions of the parameters in these two classes are not known. If the parameters are assumed to be mostly limited within the interval (mean ± standard deviation) then a value of D_M>1 would indicate that the distribution of the features in these two classes are largely non-overlapping. However, Table 3 shows that all the features are largely overlapping and therefore none of these 11 parameters can serve as a single distinguishing feature between these two classes. Further classification was done with the help of Artificial Neural Network. Both unsupervised and supervised learning methods were employed where all the features were simultaneously used. .

Unsupervised Classification: Eleven dimensional feature vectors were pooled from both the classes (from a total of 280 sub images) separately for every pair of (NH, θ) and then SOM [35] was applied to perform an unsupervised classification. Number of input neurons was taken as eleven and initially, the number of output neurons was taken as two. The weight vectors of the output neurons after saturation became representative of the input vectors. However, it was found that, in this representation, the input vectors, which led to a given output neuron to win, did not belong to any particular class. Therefore, classification was not achieved at this stage. The number of output neurons wasgradually increased up to a value of 70. On increasing the number of output neurons it was found that few output neurons

were winner for feature vectors of only normal class while few others were winner for that of the fatty class. Let us callsuch an output neuron a pure neuron. A successful classification would mean all the output neurons are pure and an unambiguous class may be assigned to every output neuron so that a test vector can be assigned to a class from the class of the corresponding winner neuron. Number of pure neurons were less than 60% in the present study (35% fatty and 25% normal) while the rest of the output neurons (40 %) were not pure. Therefore, the unsupervised learning by SOM was not very useful for the present classification.

Supervised Classification: Next we applied a supervised learning method, namely, MLP with error back propagation learning algorithm [36]. We used 11 neurons in the input layer and a single neuron in the output layer with one hidden layer. The numbers of neurons in the hidden layer were optimized to produce best possible classification performance. Supervised classifications algorithm demands that the total data be divided into training and test set. The convention is to use large training set for an exhaustive training and consequently, the test set become small for the finiteness of the total data set. However, as an alternative, we attempted to train the network with a set which was not a part but a representative of the data. We separated the feature vectors of each class for each (NH, θ). We obtained 20 representatives of the normal vectors for a particular (NH, θ) by using them as inputs to a SOM with eleven input and 20 output neurons. A similar SOM gave us 20 representatives of the fatty vectors. These 40 representative vectors were used as the training set while the entire data set comprising 280 sub images was treated as the test set. This algorithm, denoted as representative training, was contrasted with the conventional training-test partition in 2:1 ratio. The utility of pre-processing was also explored by running the classification with and without pre-processing the input vectors by PCA. For PCA, the minimum fraction of total variation was set at 0.001 and the number of input neuron of MLP was reduced in accordance with the dimensionality of the pre-processed feature space. The classification was therefore explored with four different modes- i) Common-Conventional training and test set without pre-processing, ii) Representative – Training set generated using SOM but the input vectors were not pre-processed, iii) PCA-Commondata set with inputs pre-processed using PCA and iv) PCA Representative – SOM generated training set with inputs pre-processed.

The performance of the classification was measured by the following two parameters, namely, specificity and sensitivity (Equation 2).

$$Specificity = TN / FP + TN$$

$$Sensitivity = TP / TP + FN \quad (2)$$

Where TP is true positive (true fatty), TN true negative (true normal), FP false positive (false fatty) and FN is false negative (false normal). Since a computer aided classification should be used as a preliminary filter in the medical diagnosis, a high value of sensitivity is desirable. We used one layer of hidden neurons and the number of neurons in the hidden layer was optimized for best sensitivity.

The value of best sensitivity and corresponding specificity of different (NH, θ) using the above four methods are shown in figures 2 and 3, respectively. It is interesting to note that different (NH, θ) values fared quite differently towards classification and an averaging would mask this result. Table 2 shows the best performances in each of the four input paradigms.

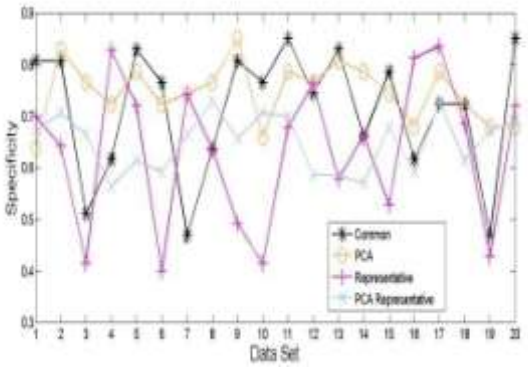

Fig 2

Figure 2 Shows specificity values at different data sets for four input paradigms. Each data set correspond to a value of NH,θ as described in table2.

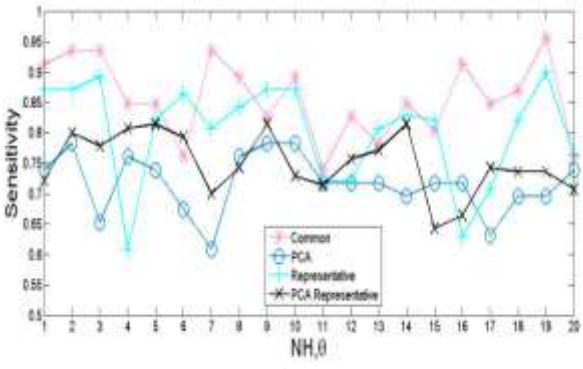

Fig. 3

Figure 3 Shows specificity values at different data sets for four input paradigms. Each data set correspond to a value of NH,θ as described in table 2.

Performance of the classifier can also be depicted as a point in the Receiver Operating Characteristic (ROC) space by plotting the fraction of true positives out of total positives (True Positive Rate) vs. the fraction of false positives out of total negative (False Positive Rate).

Evidently, these two rates are equivalent to sensitivity and (1-specificity). An ideal classification would yield these two values as 1 and 0 and therefore generate a point in the left upper corner of the ROC space.
However, a point in the bottom right corner is equally acceptable, but in the latter case the decision of the classifier has to be accepted with a NOT. The origin passing diagonal is a line of no discrimination since for any point on this line rate of true positive is equal to the rate of false positive. Therefore, the perpendicular distance of the point from the no discrimination line gives a single valued score to rank the performance of a classifier. Figure 4 shows two best points in the ROC space in each of the modes. Clearly, the common mode (Conventional training-test partition without pre

Table 4 Shows best classification performance for each of the four modes. Results with maximum sensitivity are reported.

Mode	Best value of sensitivity	Corres-ponding specificity	Corres-ponding NH, θ
Common Representative PCA PCA-Representative	0.94 0.87 0.78 0.8	0.81 0.7 0.85 0.71	1, 0 1, 45 3,0 1,0

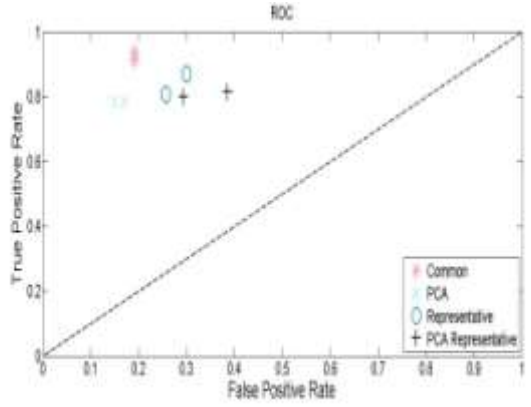

Fig. 4

Figure 4 plots of false positive rate vs. true positive rate of two best results for each of four input paradigms. The dashed line represents the line of no discrimination.

Processing yields best result. PCA increases the specificity marginally but reduces the sensitivity markedly. The best results for each of the four modes are tabulated in table 4.

4. CONCLUSION

In this study we attempted to establish Computer Aided Diagnosis tool for identifying the diseased (fatty) and control (normal) human livers from USG images. For this purpose unsupervised (using SOM) and supervised (using MLP) neural network were used as classifiers. SOM did not give satisfactory classification. To get better classification MLP learning algorithm was used. For classification, training and test data set were built with original features values and as well as pre-processed feature values. From this study we found the performance with original feature values was better than with pre-processed values. The training data set was built in two ways - one was uniform selection of two third data (Common) and another was by selecting representatives. Here we saw that common training data set gave better result compared to representative training data set. However the performance measurement was more reliable if the test data set was large. The representative training algorithm makes the test set large and hence it was worth to explore in future if, with other choice of classifiers, this algorithm would lead better accuracy.

ACKNOWLEDGMENT

We would like to thank Dr.SuparnaMajumdar, Department of Radiodiagnosis, Chittaranjan National Cancer Institute, Kolkata-700026, India, for providing the USG of livers for this study.
Table 3 shows the $D_m$values of different features at different NH and θ. Values were less than 1 indicating the distribution of the features from normal and fatty classes were overlapping (see text for explanation).

NH,θ	MAXP	ASM	ENT	IKMOM	HOMO	CONTRAST	CORR	IDM	SHADE	PROM	VAR
1,0	0.073512	0.182194	0.21552	0.129162	0.071002	0.131335	0.498241	0.071171	0.125531	0.214	0.32197
1,45	0.141674	0.226449	0.28347	0.347281	0.210572	0.22036	0.45839	0.222174	0.109021	0.01344	0.14561
1,90	0.104131	0.185033	0.19656	0.158229	0.139174	0.1866	0.456505	0.136468	0.092215	0.040612	0.13959
1,135	0.156997	0.232843	0.25499	0.24532	0.238959	0.22947	0.456783	0.238867	0.075934	0.036227	0.14293
2,0	0.132701	0.232389	0.26344	0.274052	0.231834	0.26554	0.459008	0.231802	0.101205	0.030777	0.14909
2,45	0.120465	0.214668	0.20896	0.198837	0.186117	0.14843	0.456086	0.189972	0.037714	0.003335	0.14235
2,90	0.10975	0.214105	0.21934	0.224497	0.20244	0.20233	0.455016	0.203015	0.059099	0.065353	0.13614
2,135	0.155776	0.232329	0.23648	0.271644	0.240723	0.22467	0.455672	0.242663	0.04267	0.04109	0.14388
3,0	0.136113	0.232089	0.24249	0.234038	0.229693	0.25273	0.459959	0.226345	0.083673	0.035197	0.15019
3,45	0.152545	0.219136	0.2113	0.202802	0.227405	0.1748	0.45534	0.227318	0.042496	0.013767	0.13951
3,90	0.146683	0.22517	0.22613	0.24814	0.263585	0.22624	0.453249	0.264312	0.048439	0.074986	0.13237
3,135	0.119304	0.22045	0.221	0.231692	0.235995	0.20724	0.454318	0.236497	0.033781	0.03339	0.14067
4,0	0.148501	0.228012	0.22473	0.203062	0.209879	0.22149	0.460711	0.206873	0.079461	0.028623	0.152
4,45	0.102807	0.211998	0.20015	0.243624	0.224852	0.18548	0.455079	0.227227	0.060227	0.014193	0.1366
4,90	0.140721	0.225649	0.21985	0.232892	0.259133	0.21453	0.451762	0.258917	0.056922	0.077786	0.12814
4,135	0.135005	0.218732	0.21264	0.288737	0.237567	0.23339	0.452718	0.241117	0.032483	0.048384	0.13671
8,0	0.131382	0.22345	0.20456	0.126284	0.132721	0.1276	0.464001	0.130162	0.067423	0.01591	0.16072
8,45	0.133559	0.2013	0.18008	0.249383	0.226624	0.14614	0.458111	0.236009	0.0929	0.02268	0.14225
8,90	0.199744	0.216268	0.19259	0.292234	0.320755	0.23039	0.448694	0.326221	0.063359	0.061486	0.12026
8,135	0.114664	0.19887	0.17133	0.264123	0.251097	0.23866	0.450698	0.251267	0.033053	0.065671	0.13463

REFERENCE

[1] D. Jirak, M. Dezortova, P. Taimr, M. Hajek ," Texture analysis of human liver", Magnetic and Resonance Imaging, vol. 15 , pp. 68-74, 2002.

[2] D. Gaitini, M. Lederman, Y. Baruch, E. Ghersin, E. Veitsman, H. Kerner et al.," Computerised Analysis of Liver Texture with Correlation to Needle Biopsy", Ultraschall in Med, vol. 26, pp. 197-202, 2005.

[3] K. Ogawa, M. Fukushima, K. Kubuta, N. Hisa," Computer Aided Diagnosis System for Diffuse Liver Diseases with Ultrasonography by Neural Networks", IEEE transactions on Nuclear Science vol. 45, pp. 3069-3074, 1998.

[4] W.C. Yeh, S.W. Huang, P.C. Li,"Liver Fibrosis Grade ClassificationWith B-Mode Ultrasound", Ultrasound in Medicine and Biology vol. 29, pp.1229-1235, 2003.

[5] Z. Jiang, K. Yamauchi, K. Yoshioka, K. Aoki, S. Kuroyanagi, A. Iwata, et al.," Support Vector Machine-Based Feature Selection for Classification of Liver Fibrosis Grade in Chronic Hepatitis C", Med Sys vol:30 pp: 389-394,2006.

[6] S. Poonguzhali, G. Ravindran ," Automatic Classification of Focal Lesions in Ultrasound Liver Images Using Combined Texture Features", Information Technology ,vol:7, pp. 205-209,2008.

[7] D. S. Elizabeth, A. Kannan, H. K. Nehemiah, "Computer-aided diagnosis system for the detection of bronchiectasis in chest computed tomography images", Imaging Systems and Technology , vol. 19,pp. 290-298,2009.

[8] X. Liu. J. Liu. D. Zhou. J.Tang. "A Benign and Malignant Mass Classification Algorithm Based on an Improved Level Set Segmentation and Texture Feature Analysis". 4th International Conference on Bioinformatics and Biomedical Engineering (iCBBE) 2010.

[9] G. Li, Y. Luo, W. Deng, X. Xu, A. Liu, E. Song ,"Computer Aided Diagnosis of Fatty Liver Ultrasonic Images Based on Support Vector Machine", Proceedings of the 30th Annual International IEEE Engineering in Medicine & Biology Society Conference, pp. 4768 – 4771,2008.

[10] D. Mittal, V. Kumar, S.C. Saxena, N. Khandelwal, N. Kalra, "Neural network based focal liver lesion diagnosis using ultrasound images ",Computerized Medical Imaging and Graphics, vol. 35, pp. 315-323,2011.

[11] M.S. Gebbinck, J.T.M. Verhoeven, , J.M. Thijssen, T.E.Schouten ,"Application of Neural Networks for the Classification of Diffuse Liver Disease by Quantitative Echography", Ultrasonic Imaging, vol.15, pp. 205-217,1993.

[12] W.L. Lee, Y.C. Chen, K.S. Hsieh ," Ultrasonic liver tissues classification by fractal feature vector based on M-band wavelet transform", IEEE Transactions on Medical Imaging , vol. 22 ,pp. 382-392 ,2003.

[13] S. Moldovanu, L. Moraru, D. Bibicu," Computerized decision support in liver steatosisinvestigation",Biology And Biomedical Engineering , vol. 6, pp. 69-76,2012.

[14] D. Gaitini, Y. Baruch, E. Ghersin, E. Veitsman, H. Kerner, B. Shalem, et al. ," Feasibility Study of Ultrasonic fatty Liver Biopsy: Texture vs. Attenuation and Backscatter", Ultrasound in medicine and biology, vol. 30, pp. 1321-1327, 2004.

[15] D.R. Chen, R.F. Chang, C.J. Chen, M.F. Ho, S.J. Kuo, S.T. Chen, et al.," Classification of breast ultrasound images using fractal feature", Clinical Imaging, vol. 29, pp.235-245, 2005.

[16] K.H. Hwang, J.G. Lee, J.H. Kim, H.J. Lee, K.S. Om, M. Yoon, et al. , "Computer Aided Diagnosis (CAD) of Breast Mass on Ultrasonography and Scintimammography", Proceedings of 7th International Workshop on Enterprise networking and Computing in Healthcare Industry, pp.187-189, 2005.

[17] M.H. Horng,"Texture Characteristic for Classification of the Ultrasonic Images of Rotator Cuff Diseases",International Conference on BioMedical Engineering and Informatics, vol. 2, pp. 258-262, 2008.

[18] D.G. Vince, K.J. Dixon, R.M. Cothren, J.F. Cornhill, "Comparison of texture analysis methods for the characterization of coronary plaques in intravascular ultrasound images .",Computerized Medical Imaging and Graphics ,vol. 24 ,pp. 221-229,2002.

[19] P.A. Linares, P.J. McCullagh, N.D. Black, J. Dornan, "Feature selection for the characterization of ultrasonic images of the placenta using texture classification", IEEE International Symposium on of Biomedical Imaging: Nano to Macro , vol. 2, pp. 1147-1150, 2004.

[20] G. Malathi and V. Shanthi ,"Histogram Based Classification of Ultrasound Images of Placenta", Computer Applications, vol.1 , pp. 49-53,2010.

[21] A.S.M. Sohail, M.M. Raheman, P. Bhattacharya, S. Krishnamurthy, S.P. Mudur " Retrieval and classification of ultrasound images of ovarian cysts combining texture features and histogram moments", IEEE International Symposium on Biomedical Imaging: From Nano to Macro , pp. 288-291,2010.

[22] N.N. Tsiaparas, S. Golemati, I. Andreadis, J.S. Stoitsis, I. Valavanis, K.S. Nikita, "Comparison of Multi resolution Features for Texture Classification of Carotid Atherosclerosis From B-Mode ultrasound", IEEE Transactions on Information Technology in Biomedicine , vol. 15 , pp. 130-137,2011.

[23] W. Qiu, F. Xiao, X. Yang, X. Zhang, M. Yuchi, M. Ding, " Research on Fuzzy Enhancement in the Diagnosis of Liver Tumor from B-mode Ultrasound Images", Image, Graphics and Signal Processing ,vol. 3, pp. 10-16,2011.

[24] G. T. Cao, P. Shi, B. Hu," Liver fibrosis identification based on ultrasound images captured under varied imaging protocols", J Zhejiang University Science, vol.6 , pp.1107-1114,2005.

[25] C.I. Christodoulou, C.S. Pattichis, M. Pantziaris, A. Nicolaides ,"Texture-Based Classification of Atherosclerotic Carotid Plaques", IEEE Transactions On Medical Imaging, vol. 22, pp. 902-912, 2003.

[26] V.E. Salca, M. Gordan, A. Vlaicu ,"A Multi-level Voting Scheme of Kernel Fisher Discriminant Classifiers for Liver Fibrosis Identification in Ultrasound Images",Proceedings in Applied Mathametics and Mechanics ,vol. 11, pp. 861-862, 2011.

[27] R.M. Haralick, K. Shanmugam, Dinstein , Textural features for image classification. IEEE Transaction on Systems Man and Cybernetics, vol.3, pp. 610-21, 1973.

[28] R. F. Walker, P. Jackway, I.D. Longstaff ,"Improving Co-occurrence Feature Discrimination ", 3rd conference on digital image computing: techniques and applications , pp.643-648, 1995.

[29] D. A. Clausi."Texture segmentation of SAR sea ice imagery". Ph.D. dissertation .Waterloo Univ.. Waterloo Ont..Canada.1996.

[30] Z. Y. Tau. Y.L. Phooi. H.T. Wang. "Computer vision-based wood recognition system".Proc.Of International workshop on Advance Image technology, 2007.

[31] N. V. Chawla, K. W. Bowyer, L. O. Holl, W. P. Kegelmeyer ,"SMOTE: Synthetic Minority Over-sampling Technique", Artificial Intelligence Research , vol.16, pp. 321-357,2002.

[32] I. Valavanis, S. G. Mougiakakou, K.S. Nikita, A. Nikita, "Computer aided diagnosis of CT focal liver lesions by an ensemble of neural network and statistical classifiers", IEEE International Joint Conference on Neural Networks ,vol. 3, pp. 1929-1934, 2004.

[33] B. Liu, H.D. Cheng, J. Huang, J. Tian, X. Tang, J. Liu ,"Fully automatic and segmentation-robust classification of breast tumors based on local texture analysis of ultrasound images", Pattern Recognition , vol. 33, pp. 280-298, 2010.

[34] M. Gletsos, S.G. Mougiakakou, G.K. Matsopoulos, K.S. Nikita, A.S. Nikita, D. Kelekis," A Computer-Aided Diagnostic System to Characterize CT Focal Liver Lesions: Design and Optimization of a Neural Network Classifier",

IEEE transactions on information technology in biomedicine ,vol. 7, pp.153-162, 2003.

[35] T. Kohonen, "Self-organized formation of topologically correct feature maps", Biological Cybernetics , vol. 43, pp.59-69,1982.

[36] D.E. Rumelhart, G.E. Hinton, R.J. Williams, "Learning representations by back-propagating errors", Nature , vol. 323, pp. 533–536,1986.

AUTHOR'S PROFILE

NiveditaNeogi received M.E. degree in Information Technology from West Bengal University of Technology ,West Bengal,India in 2007. She is persuing the Ph.D. degree in Computer Science from West Bengal State University ,West Bengal,India.

Now she is Assistant Professor in the department of Information Technology at Meghnad Saha Institute of Technology(Techno India Group),Kolkata,India.

Her research interest area is image processing, texture analysis and pattern recognition.

ArunabhaAdhikari, Ph.D. obtained his masters in Physics from Calcutta University in Physics. He worked in Saha Institute of Nuclear Physics as a senior research fellow and obtained doctoral degree from Calcutta University. His initial research was in Biophysics. Topic of his Ph.D. research was related to theoretical simulation of Calcium Action Potential. Later we worked in the laboratories of electrophysiology in Indian Institute of Science, Bangalore, India and Department of Physiology, University of Saarland, Germany. He has been teaching physics for the last 17 years and presently working in the West Bengal State University. His present interests concern computational physics, computational neuroscience and application of neural network in biomedical image processing.

Madhusudan Roy, Ph.D. obtained his masters in Physics and Ph. D. degree from the North Bengal University in 1983 and 1989 respectively. He has been working in the fields of material science, gas sensors, photoacoustic imaging, image analysis. Presently, he is working in Saha Institute of Nuclear Physics, Kolkata, India.